2019

A magnetorheological elastomer rail damper for wideband attenuation of rail noise and vibration

Shuaishuai Sun
University of Wollongong, Tohoku University, ssun@uow.edu.au

Jian Yang
University of Wollongong, University of Science and Technology of China, yangj@uow.edu.au

Tanju Yildirim
Shenzhen University, ty370@uowmail.edu.au

Donghong Ning
University of Wollongong, dning@uow.edu.au

Xiaojing Zhu
University of Wollongong, xz979@uowmail.edu.au

See next page for additional authors

A magnetorheological elastomer rail damper for wideband attenuation of rail noise and vibration

Abstract

The noise and vibration effects of rails can have a significant impact on the environment surrounding the railways. Rail dampers are elements that are attached to the sides of the rail and can improve the track decay rate of rail and then enhance the rails' ability to attenuate noises and vibrations. However, in practical applications, the most efficient rail damper design still cannot adjust its own parameters to adapt to different requirements because their stiffness and damping are fixed after designed. In this work, a tunable magnetorheological elastomer rail damper that works on the principle of a dynamic vibration absorber has been designed, analysed, characterised, and experimentally tested for the suppression of railway noise and vibration. The new rail damper incorporates variable stiffness magnetorheological elastomer layers, whose stiffness can be controlled by an externally applied magnetic field, to realise adaptive characteristics. Experimental characterisations of the magnetorheological elastomer rail damper were performed with an electromagnetic shaker. Subsequently, theoretical predictions of the track decay rate of a UIC-60 rail with different rail dampers and without rail damper were conducted; simulation results verified that magnetorheological elastomer rail dampers can improve the track decay rate of rail over a wider frequency range compared to conventional rail dampers and thus the performance of the magnetorheological elastomer rail damper outperforms other conventional rail dampers on rail noise reduction.

Disciplines

Engineering | Science and Technology Studies

Publication Details

Sun, S., Yang, J., Yildirim, T., Ning, D., Zhu, X., Du, H., Zhang, S., Nakano, M. & Li, W. (2019). A magnetorheological elastomer rail damper for wideband attenuation of rail noise and vibration. Journal of Intelligent Material Systems and Structures, Online First 1-9.

Authors

Shuaishuai Sun, Jian Yang, Tanju Yildirim, Donghong Ning, Xiaojing Zhu, Haiping Du, Shiwu Zhang, Masami Nakano, and Weihua Li

Published as:
Sun, S., Yang, J., Yildirim, T., Ning, D., Zhu, X., Du, H., Zhang, S., Nakano, M. & Li, W. (2019). A magnetorheological elastomer rail damper for wideband attenuation of rail noise and vibration. *Journal of Intelligent Material Systems and Structures, Online First 1-9.*

An MRE rail damper for wideband attenuation of rail noise and vibration

S.S. Sun[1,5*], J. Yang[1,2], T. Yildirim[3], D. Ning[4], X. Zhu[1], H. Du[4], S.W. Zhang[2*],

M. Nakano[5] and W.H. Li[1]

[1]School of Mechanical, Materials, Mechatronic and Biomedical Engineering, University of Wollongong, New South Wales 2522, Australia
[2] Department of Precision Machinery and Precision Instrumentation, University of Science and Technology of China, Hefei, Anhui province 230026, China
[3] Guangdong Provincial Key Laboratory of Micro/Nano Optomechatronics Engineering, College of Chemistry and Environmental Engineering, Shenzhen University, Shenzhen, Guangdong, China
[4] School of Electrical, Computer & Telecommunications Engineering, University of Wollongong, New South Wales 2522, Australia
[5]New Industry Creation Hatchery Center (NICHe), Tohoku University, Sendai, Miyagi, 980-8577, Japan.
*Corresponding authors: ssun@uow.edu.au, swzhang@ustc.edu.cn

Abstract

The noise and vibration effects of rails can have a significant impact on the environment surrounding the railways. Rail dampers are elements that are attached to the sides of the rail and can improve the track decay rate (TDR) of rail and then enhance the rails' ability to attenuate noises and vibrations. However, in practical applications, the most efficient rail damper design still cannot adjust its own parameters to adapt to different requirements because their stiffness and damping are fixed after designed. In this work, a tuneable magnetorheological elastomer (MRE) rail damper that works on the principle of a dynamic vibration absorber (DVA) has been designed, analysed, characterised, and experimentally tested for the suppression of railway noise and vibration. The new rail damper incorporates variable stiffness MRE layers, whose stiffness can be controlled by an externally applied magnetic field, to realise adaptive characteristics. Experimental characterisations of the MRE rail damper were performed with an electromagnetic shaker. Subsequently theoretical predictions of the TDR of a UIC-60 rail with different rail dampers and without rail damper were conducted; simulation results verified that MRE rail dampers can improve the TDR of rail over a wider frequency range compared to conventional rail dampers and thus the performance of the MRE rail damper outperform other conventional rail dampers on rail noise reduction.

Keywords: Magneto-rheological elastomer; Rolling noise; Rail damper; Vibration and noise attenuation; Tuneable frequency

1. Introduction

A systematic approach to the control of railway noise and vibration, requires separating the individual contribution of each noise source along the track to identify the most dominant contributor to the overall noise spectrum [1]. The wayside noise emitted by a railway system is known to be a combination of different sources caused by several different mechanisms, such as, rolling noise, curve squeal, ground vibration and aerodynamic noise; depending on the situation and frequency of excitation; different mechanisms are more dominant than others in certain frequency ranges. However, the most dominant source of noise is rolling noise generated from the wheel/rail interface and the vibrations induced into wheel and rail components from surface irregularities. The roughness between running surfaces results in vertical and lateral vibration of the wheel and rail according to their dynamic interaction properties. Subsequently these vibrations lead to the wheel and track structures radiating sound power [2, 3]. Many solutions for reducing railway noise are available commercially varying from damping treatments, grinding, vibration isolation, acoustic absorption and shielding. Nevertheless, noise and vibration control at the source of the noise is often the most cost effective and efficient option [4]. One prominent solution to minimise railway rolling noise is rail dampers; these devices work on the principle of a dynamic vibration absorber (DVA), where the resonance frequency of the device is selected to match the dominant frequency of the vibration and sound spectrum in order to transfer the vibration energy in the rail at this frequency to the rail damper. The rail damper operates by enhancing the attenuation of vibration transmitted along the rail with distance and thus suppress the rail noise; the track decay rate is used to measure and quantify the reduction of the rail noise and vibration by the rail dampers [5]. The higher the track decay rate, the better performance of the rail damper on rail noise reduction. Several different rail dampers have been designed and manufactured in the past decades. For the rail dampers, more oscillating masses designed inside the damper means more resonances and better performance. However, more oscillating masses also complicate the rail damper system and enhance the cost. To balance the effectiveness of the rail damper and its complexity and cost, two masses system has been chosen and wildly used nowadays [6]. Unfortunately, as the natural frequencies of the traditional rail dampers are fixed, they cannot adapt to the variation of excitation frequency because of different trains and different train operation speeds. This limitation has restricted the effectiveness of rail dampers to achieve maximum noise reduction over a wider frequency range. Hence, its efficiency in reducing rolling noise is limited due to its narrow effective frequency bandwidth.

A novel approach to provide continuous tuning frequencies and adaptability is the integration of magneto-rheological (MR) elastomer (MRE) materials into a rail damper system. MREs are a group of smart materials [7-10] that have field dependent 'rheological' properties; these properties, give these materials tuneable stiffness and damping attributes. Although there is a vast range of MR materials with variable matrix compositions; MR elastomers, produced with an elastomer matrix, have extensively been utilised in variable stiffness applications, notably vibration absorbers [11-13] and isolators [14-17]. For example, Ginder, et al. [18, 19] did pioneer research and designed a tuned vibration absorber (TVA) with MRE that was able to have frequency adaptability. Lerner and Cunefare [20] investigated the vibration absorption characteristics and field dependence of an MRE vibration absorber; different working modes of the MRE absorber were investigated, including shear, longitudinal and squeeze working modes. Deng and Gong [12] developed an adaptive tuned vibration absorber (ATVA) using MRE, which was able to shift the natural frequency of the device by over 50%, the authors note that the use of MREs to develop ATVAs may have many advantages such as rapid response, simple construction, ease of employment, good response, and efficient controllable qualities. Similar to absorbers, MRE can also extend the effective frequency bandwidth of rail dampers and greatly enhance their performance by adjusting their natural frequencies to compensate for the shift in the excitation frequency. The rail dampers integrated with MREs will have a substantial advantage in terms of controlling the device's natural frequency across a wide range of frequency bands of interest.

In this work, an adaptive rail damper based on MREs has been designed, prototyped, experimentally characterised and its effectiveness on vibration and noise suppression of railway has been numerically analysed and verified. A rail damper with two effective masses, two MRE layers and two embedded coils has been designed. The stiffness of the MRE layers can be controlled by adjusting the coils' current so as to achieve a tuneable rail damper. The work has been organised as follows; Section 2 describes the design and analysis of the MRE-based rail damper; Section 3 conducts the frequency shift testing of the fabricated device and its parameter identification; Section 4 gives an in-depth analysis on increasing the railway's track decay rate with MRE rail dampers and Section 5 ends with concluding remarks.

2. Design and analysis of the MRE-based rail damper

In this section, a detailed description on the design and working principle of the MRE-based rail damper has been presented; moreover, COMSOL Multiphysics simulations have been used to analyse the magnetic strength of the fabricated device.

2.1. Design and working principle of the MRE-based rail damper

The working principle of a rail damper is that the vibration energy of the railway would be

transferred to the rail damper when the natural frequency of rail damper matches the vibration frequency of rail. For conventional rail dampers, their working frequency range is narrow and only works effectively around a small frequency range. In order to expand the working frequency range of the conventional rail dampers, the application of MRE materials to develop adaptive rail damper is an ideal solution because the stiffness of MRE is controllable and thus the natural frequency of the rail damper can be controlled to achieve a broadband effective frequency range. Figure 1 (a) illustrates the schematic of the design of the rail damper with two MRE sheets, as well as, the magnetic closed loop circuits. The rail damper consists of four main parts as shown in Figure 1(b), the steel masses representing the effective masses, the MRE layers acting as springs with a variable stiffness, the coils providing controllable magnetic flux density and the plastic plate offering a uniform surface to the MRE layers. From the structure of the rail damper it can be seen that the stiffness of the MRE can be controlled by the magnetic field generated by the coils. As the stiffness of the MRE determine the natural frequency of the rail damper, the resonance frequency of the MRE rail damper can be controlled by the coil current to trace the frequency variation of the rail vibration. As the noise of the rail is generated by the rail vibration, the rail noise level will be reduced after the rail vibration is attenuated. The rail damper is a 2-DOF system, which has two resonance frequencies. From the structure of the MRE rail damper, it can be seen that the magnetic field through the two MRE layers can be controlled separately by the two coils. The upper coil is defined as coil 1 and the lower coil is defined as coil 2 in the following context.

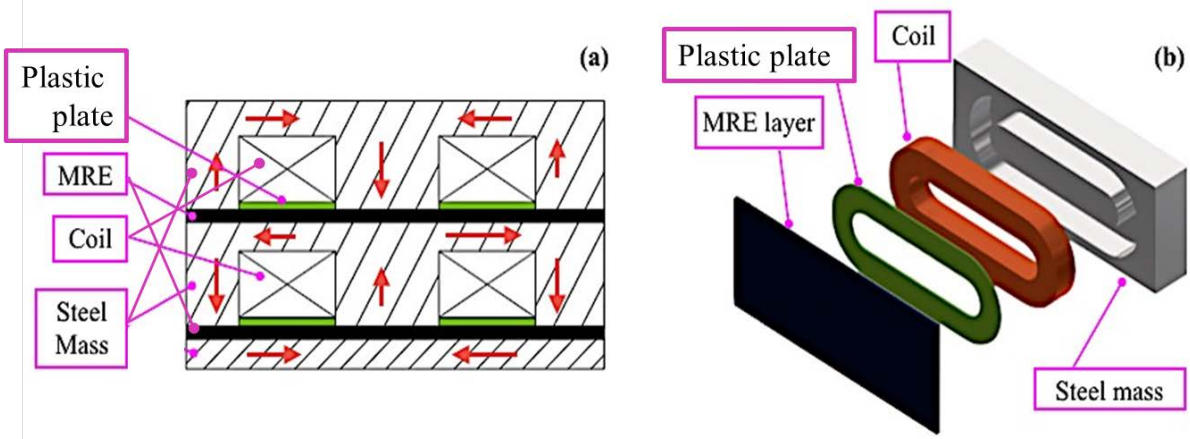

Figure 1: (a) Design of MRE rail damper; (b) MRE rail damper components (one layer)

According to the working principle of the MRE rail damper, its tuning frequency should be designed close to the frequency at which the rail vibration magnitude reaches its peak; Track wheel interaction noise software (TWINS) models estimated that this peak, for a train speed of 100 km/h is in the frequency range of 650-850Hz [21]. As there are many trains operating faster than 100 km/h, the targeted design frequency range is set to be around 800Hz-900Hz. The natural frequency of the MRE rail dampers can be calculated by the following equation

and this calculation procedure can be used to guide the design of the detailed parameters of rail damper.

The motion equation of the masses of the rail damper under acceleration excitation can be expressed as Eqn.1.

$$\mathbf{M}\ddot{\mathrm{X}}(\mathrm{t}) + (\mathbf{C}_\mathrm{s} + \Delta\mathbf{C})\dot{\mathrm{X}}(\mathrm{t}) + (\mathbf{K}_\mathrm{s} + \Delta\mathbf{K})\mathrm{X}(\mathrm{t}) = -\mathbf{M}\ddot{\mathrm{x}}_\mathrm{g} \quad (1)$$

where $\mathbf{M}$ is the mass matrices; $\mathbf{C}_\mathrm{s}$ and $\Delta\mathbf{C}$ are matrices of initial damping and damping variable controlled by magnetic field, respectively; $\mathbf{K}_\mathrm{s}$ and $\Delta\mathbf{K}$ are matrices of initial stiffness and MRE stiffness variation under different magnetic field, respectively; X(t) is a vector of the mass displacements relative to the rail excitation; $\ddot{x}_\mathrm{g}$ is the rail vibration.

The resonance frequency of the rail damper can be calculated by solving the characteristic equation of Eqn.1: $|(\mathbf{K}_\mathrm{s} + \Delta\mathbf{K}) - \omega^2\mathbf{M}| = 0$. The stiffness of MRE is determined by the young's modulus, thickness and effective area of MRE layers. As a result the natural frequency of the rail damper is determined by the mass of the oscillator, the thickness of the MRE layer, the young's modulus of the MRE materials and the effective area of the MRE layer. The mass selection of each steel mass is an important criterion for the rail damper design. As such, in the case of 2-DOF system, the upper mass of the rail damper is required to have a larger vibration frequency than the lower part so as to achieve a large frequency bandwidth. Therefore, the top mass should be smaller than the low mass. Considering all these factors and the design aim of matching the targeted frequency range, the key parameters of the rail damper are calculated and illustrated in table 1.

Table 1: Parameters of the MRE rail damper

Parameters	**Values**
Mass of the upper steel mass	0.7kg
Mass of the lower steel mass	1.1kg
The dimension of the MRE layer	60*120*2 mm
Coil turns	500

2.2. Magnetic field analysis

To take full benefit of the MRE materials, a suitable magnetic circuit has to be designed to obtain variable magnetic flux density under different applied currents. With the number of coil windings set to 500 turns and aiming to verify and validate the magnetic circuit of the design, COMSOL Multiphysics has been used to analyse the magnetic circuit and the magnetic flux density of the designed rail damper. Low carbon steel was selected for the iron cores, and its relative permeability was based on BH curves from the materials library provided within the multiphysics software. The remaining components, including air, copper wire and the plastic plate, were all given a relative permeability value of 1. The permeability of the MRE layer was selected to be 3.7 and this value was adapted from the work of

Schubert and Harrison [22], who reported the permeability of isotropic and anisotropic MRE with different compositions. The four pictures in Figure 2 shows the simulation results with both coil currents setting to 0.5A, 1A, 1.5 A and 2A, respectively. Table 2 illustrates the simulation results of the magnetic flux density across MRE layers. Referring to Figure 2, a flux density peak of 0.65T through the MRE layer at 2A could be obtained, which is high enough for controlling the rail damper. The magnetic circuits have also been presented in Figure 2(a). From this figure, it can be seen that the magnetic fields generated by the two coils are independent to each other and thus the resonances of the two mass-rubber layers can be controlled separately by the two coil currents.

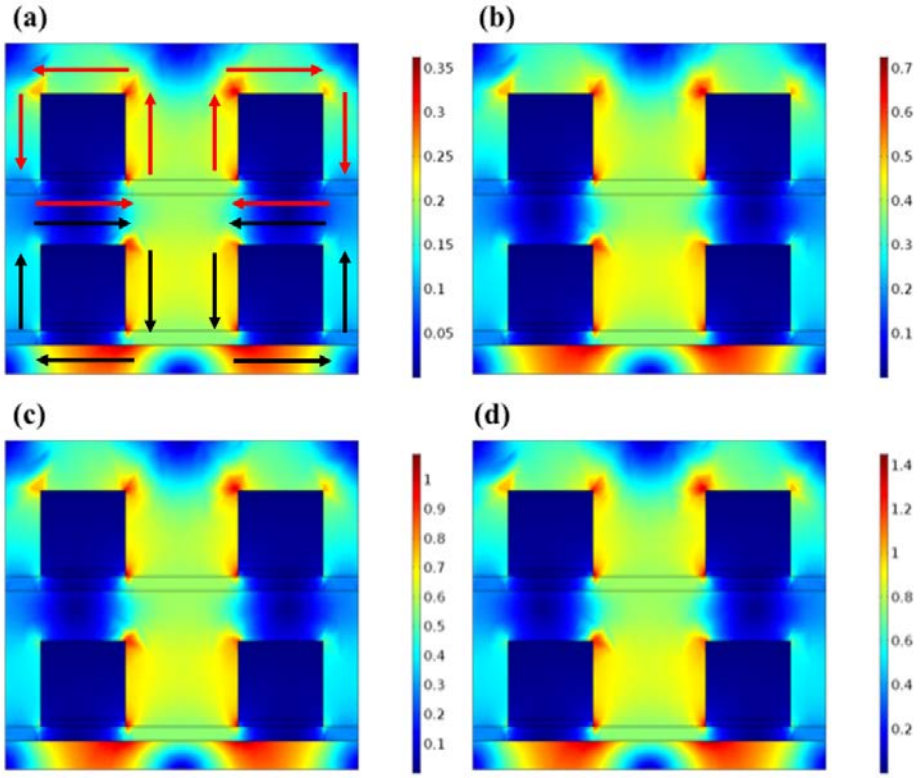

Figure 2: Magnetic field simulation with both coils' currents set to (a) 0.5 A, (b) 1.0 A, (c) 1.5 A, (d) 2.0 A

Table 2: Average flux densities through a 2 mm MRE layer

Current (A)	**Flux Density (T)**
0.5	0.16
1	0.32
1.5	0.49
2	0.65

2.3. Prototyping of the MRE-based rail damper

The first step to build the MRE rail damper is to fabricate MREs. The raw materials used in fabricating the MRE samples were silicone rubber (Selleys Pty. Ltd.) and carbonyl iron particles (C3518, Sigma-Aldrich Pty. Ltd.) with an average particle size of 5μm. Each fabricated MRE sheet had a composition ratio of the following, 7.5:2.5 of carbonyl-iron particles and silicone rubber. The two ingredients were sufficiently mixed in a beaker for about 15 minutes. Then the mixture was placed in a vacuum chamber for another 15 mins, and then moulded into a sheet to cure for a period of 48 hours at room temperature prior to testing. The plastic plates were placed on top of the coil in the final assembly to provide the necessary even surface for the MRE sheet. These holding plates were made with an interference fit so they can be tightly fitted into the slots. The coil winding was completed manually achieving 500 turns using a copper wire with a 0.5mm diameter. The prototyped rail dampers are shown in Figure 3.

3. Property testing of the MRE-based rail damper

3.1. Frequency shift property testing

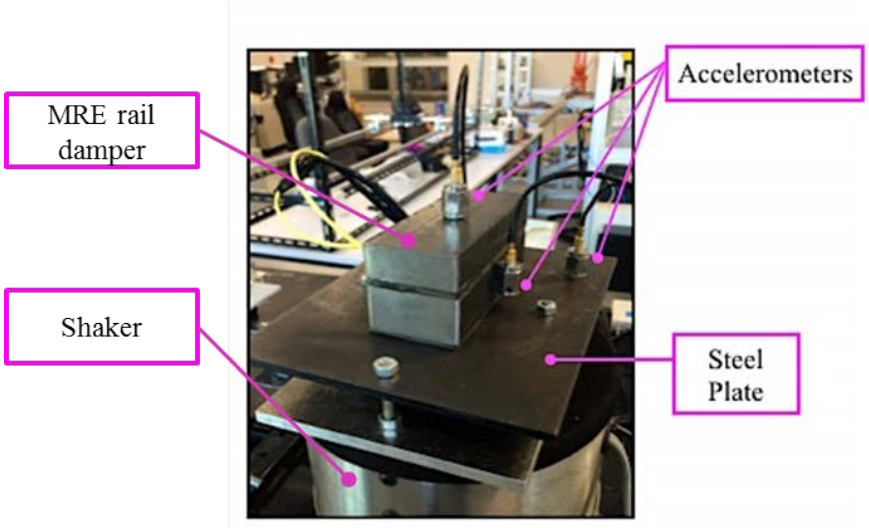

Figure 3: Frequency shift experimental setup

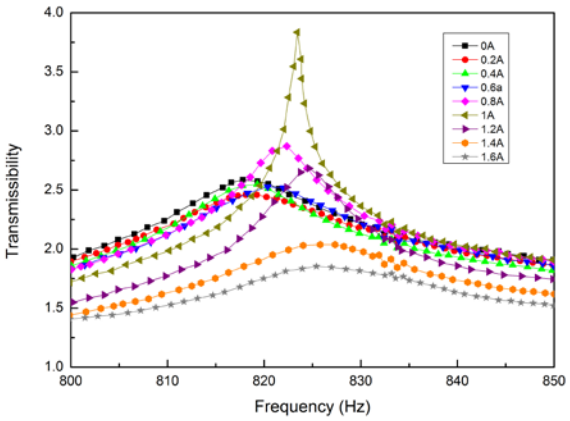

(a) Transmissibility from bottom plate to the lower mass

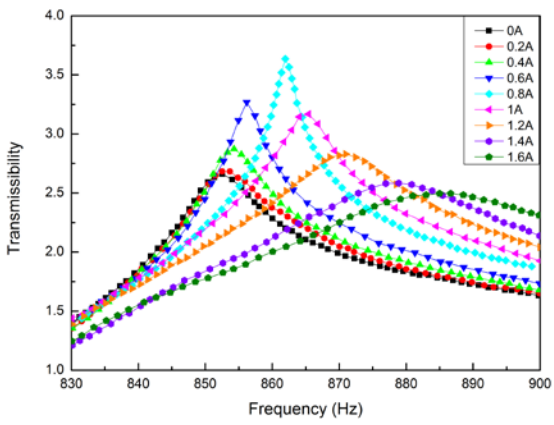

(b) Transmissibility from lower mass to the upper mass

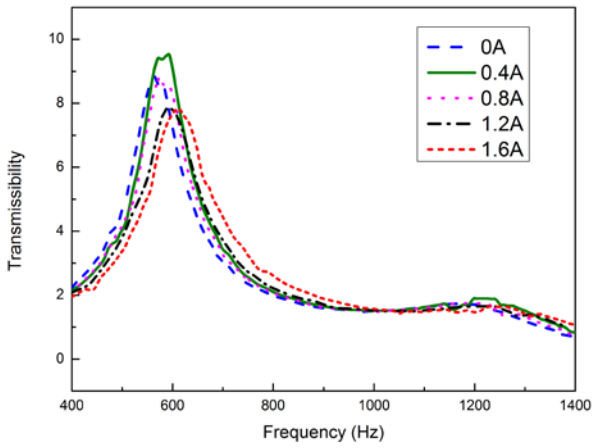

(c) Transmissibility from bottom plate to the whole rail damper

Figure 4. Transmissibility of the rail damper

The experimental setup to conduct the frequency shift test of the MR rail damper consists of the MRE-based rail damper, an electromagnetic shaker and a horizontal steel base plate, as shown in Figure 3. A base plate was attached to the shaker with four bolts to support the rail damper. The MRE-based rail damper was tested under a frequency sweep harmonic excitation generated by the shaker. The shaker is controlled by a LabVIEW program. The wires from the solenoid coil of the rail damper were connected to a DC power supply (Thurlby-Thandar, Instruments Ltd). Thus the property of the MRE rail damper can be controlled. Three accelerometers were used to measure the vibrations of each component of the rail damper, and they were placed on the upper mass, lower mass and the steel plate attached to the shaker as shown in Figure 3. The dual usage of the two accelerometers on the upper mass and the lower mass can measure the vibration transmissibility from the lower mass to the upper mass; similarly, the two accelerometers on the lower mass and the steel plate can be used to test the vibration transmissibility from the steel plate to the lower mass (with the upper mass being removed during the test), and the two accelerometers on the bottom plate and the upper mass can be used to test the transmissibility of the whole rail

damper from bottom plate to the upper mass.

In this experiment, the electrodynamic shaker was driven by a chirped frequency signal varying from 830Hz to 900Hz for the lower mass to upper mass transmissibility test and 800Hz to 850Hz for the steel plate to lower transmissibility test, respectively. As the magnetic flux density through the MRE layers can be controlled separately by the two coils, the transmissibility from bottom plate to the lower mass and from lower mass to upper mass under different excitation currents are tested individually. The experimental testing results are presented in Figures 4. The testing result shows that the natural frequency of the upper mass-spring system increased from 851Hz to 888Hz when the current of coil 1changed from 0A to1.6A; while for the lower mass-spring system, its natural frequency varied from 816Hz to 828Hz when the current of coil 2 changed from 0A to1.6A. After the individual tests of the two MRE-mass systems, the transmissibility of the whole rail damper from the bottom plate to the upper mass is also tested under a harmonic excitation with frequency sweeping from 400Hz to 1400Hz. The currents, 0A, 0.4A, 0.8A, 1.2A and 1.6A are applied to both coils during each test. The testing results, as shown in Figure 4(c), are similar with the individual tests except that there are two peaks in each result because the whole rail damper is a 2DOF system. From the testing results, it can be seen that the two resonances of the rail damper can be controlled by the current of the two coils separately. In addition, the resonance frequency range of the rail damper matches the targeted frequency range and satisfies the requirement of the rail noise reduction.

3.2. Stiffness identification of the MRE layers under different current

The stiffness and damping of the MRE layers under different currents are key parameters for the numerical analyses in the following section to evaluate the noise and vibration reduction performance of the MRE rail damper. The stiffness and damping of the MRE layers under different currents can be identified according to its experimentally obtained frequency shift performance in Fig. 4 by using the least-square method in combination with the trust-region-reflective algorithm available in MATLAB (R2013b) [23]. The identification results are illustrated in Table 3.These parameters will be used to evaluate the performance of the MRE rail damper on railway vibration and noise reduction in the following section.

Table 3: Estimated effective stiffness and equivalent damping of the MRE-based rail damper

Coil current (A)		**0**	**0.4**	**0.8**	**1.2**	**1.6**
Upper MRE layer	Stiffness (MN/m)	24.1	25.2	27.1	28.9	31.2
	Damping (kN.s/m)	6.1	6.3	6.7	7.4	8.1
Lower MRE layer	Stiffness (MN/m)	35.2	35.8	37.7	39.1	41
	Damping (kN.s/m)	9.6	10.2	10.5	11	12.1

4. Numerical evaluation of MRE-based rail damper in attenuating railway vibration and noise

4.1. Theoretical modeling of the rail treated with rail damper

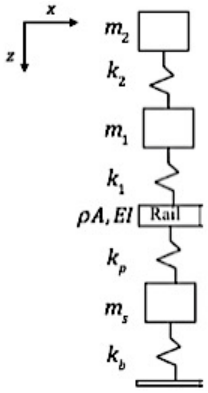

Figure 5. Continuous rail model with continuous rail damper [24]

After the development and testing of the rail damper presented in the above sections, the capability of the rail damper to attenuate the rail noise and vibration is the final key evaluation of the rail damper. In this section, numerical evaluation of the MRE rail damper on rail noise reduction is conducted and the decay rate is used to quantify its performance. The track decay rate (TDR) has been widely used to describe the attenuation of the vibration along the track for rolling noise applications and has been widely considered as a criterion in assessing rolling noise suppression capability of rail dampers [5]. The track decay rate can assess the level of damping within the track structure and therefore the noise emission from the vibrating rail in the track system [25]. The Decay rate measures the level of attenuation for the structural wave propagation within the track. For low damping values, the decay rate is low and similarly, the decay rate increases when the damping in the rail increases [26].

To determine the track decay rate of an operational railway, it is essential to include the rail pads, sleepers and ballast in the modelling. In this section, a continuous model, including rail damper, rail, rail pads, sleepers and ballast, is built, as shown in figure 5, where the rail is treated as a widely used 'Timoshenko' beam model sitting on a spring-mass-spring foundation. The pad stiffness is $k_p = 200MN/m^2$, sleeper mass is $m_s = 270kg/m$ and ballast stiffness is $k_b = 83.3MN/m^2$. The model equations are as follow. In these equations, F is a harmonic force with amplitude F and angular frequency ω, u represents the vertical displacement of the beam, u_s, u_1 and u_2 are the vertical displacement of the sleeper and the two masses inside the rail damper, $\emptyset$ is the rotation of the cross section of the beam due to the bending, κ is the shear coefficient, ρ is the density of the beam, A is cross-sectional area of the beam, I is the area moment of inertia of the beam, E is beam modulus of elasticity, G is the beam's shear modulus. m_1 and m_2 are the two effective masses of the rail damper, k_1, and

k_2 are the stiffness of the elastomeric layers inside the rail damper. k_1 and k_2 of the MRE layers are both stiffness complex with loss factor β and the loss factor can be calculated from the estimated stiffness and damping given in Table 3. The dimensions of the MRE layers and the masses of the oscillators are detailed in Table 1. The dynamic equations of the rail and rail damper system are [24]:

$$-\rho A\omega^2 u + GA\kappa(\phi' - u'') + k_p(u - u_s) + k_1(u - u_1) = F\delta(z) \ , \quad (2)$$

$$-\rho I\omega^2\phi + GA\kappa(\phi - u') - EI\phi'' = 0 \ , \quad (3)$$

The dynamic response of the sleeper is given by

$$-m_s\omega^2 u_s - k_p u + (k_p + k_b)u_s = 0 \ , \quad (4)$$

The matrix formulation for the frequency domain response of the rail damper can be formulated as

$$\begin{bmatrix} k_1 + k_2 - m_1\omega^2 & -k_2 \\ -k_2 & k_2 - m_2\omega^2 \end{bmatrix} \begin{Bmatrix} u_1 \\ u_2 \end{Bmatrix} = \begin{Bmatrix} k_1 \\ 0 \end{Bmatrix} u \ , \quad (5)$$

Then the following equation can be derived from the above equations:

$$-\rho A\omega^2 u + GA\kappa(\phi' - u'') + (k_s + k_a)u = F\delta(z) \ , \quad (6)$$

where the dynamic stiffness of the support and rail damper are given by

$$k_s = k_p\left(1 - \frac{k_p}{k_p + k_b - m_s\omega^2}\right) , \quad (7)$$

$$k_a = k_1\left(1 - \frac{k_1(k_2 - m_2\omega^2)}{(k_1 + k_2 - m_1\omega^2)(k_2 - m_2\omega^2) - k_2^2}\right) , \quad (8)$$

The parameters of the rail and support parameters selected for the simulation are listed in Table 4

Table 4: Track parameters used for theoretical TDR predictions

Parameter	**Value**	**Unit**
E	$2.1\text{x}10^{11}$	N/m^2
G	$0.77\text{x}10^{11}$	N/m^2
I	$30.55\text{x}10^{-6}$	m^4
A	$7.96\text{x}10^{-3}$	m^2
ρ	7850	kg/m^3
κ	0.4	N/A
Υ_p	0.2	N/A
Υ_b	1	N/A

For the rail damper, m_1 = 1.1kg and m_2 = 0.7kg for the lower mass and upper mass respectively, and the stiffness and damping values of the MRE layers in table 3 have been used in the numerical evaluation. With these parameters, the decay rate of the rail under different frequency can be calculated and are presented in the following section.

4.2. Predicted TDR of untreated rail and treated rail with rail dampers

The calculation results are presented in Figure 6. In this calculation, the rail TDR without the attachment of the rail damper is evaluated to provide as a reference for comparison. The other curves in Figure 6 are the TDR of the rail treated with the rail dampers with different constant current (both coils in the rail damper are excited with the same constant current) and controlled current. These rail dampers with different constant currents are considered as passive rail dampers with different constant resonance frequencies as comparing references. From Fig. 6 it can be seen that the TDR of the untreated rail and treated rail are high and similar before 500 Hz. This is because the rail experiences large damping from the track foundation induced by the resilient pads or the energy transmitted into the sleeper. However, this damping has slight influence on the rail decay rate when the vibration frequency of the track is greater than 500Hz. This can be evidenced by that the TDR of the untreated rail is very low after 500Hz according to Fig. 6. It can also be seen from Fig. 6 that the TDR of the rail without rail damper is much lower than the rail with rail dampers in between 800 Hz to 1200 Hz, which means the rail damper is very effective to suppress the rail noise. Looking into the performance of different passive rail dampers, it can be seen that the effective frequency range of the passive rail dampers is narrow and only effective around their renounce frequency. In addition, it also can be seen that the effective frequency range of the rail damper excited by higher current is higher, which means the effective frequency range is controllable by the current. After the evaluation of the passive rail dampers (under different constant currents), the performance of the semi-active controlled rail damper under the short-time Fourier transform (STFT) control [27] is evaluated and the TDR of the rail treated with controlled MRE rail damper is presented in Fig.6. With the STFT controller, the controlled rail damper (indicated as treated rail-variable current in Fig.6) can adjust its own resonance frequency to trace the variation of the excitation frequency to achieve a board effective bandwidth. From Fig. 6 it can be seen that the rail TDR with controlled rail damper has the maximum amplitude through the frequency range from 800-1200 Hz and it passes through almost all the maximum TDR points, indicating that this controlled rail damper is highly efficient in tracing the excitation frequency variation and outperform all other passive rail dampers regarding its vibration and noise reduction performance.

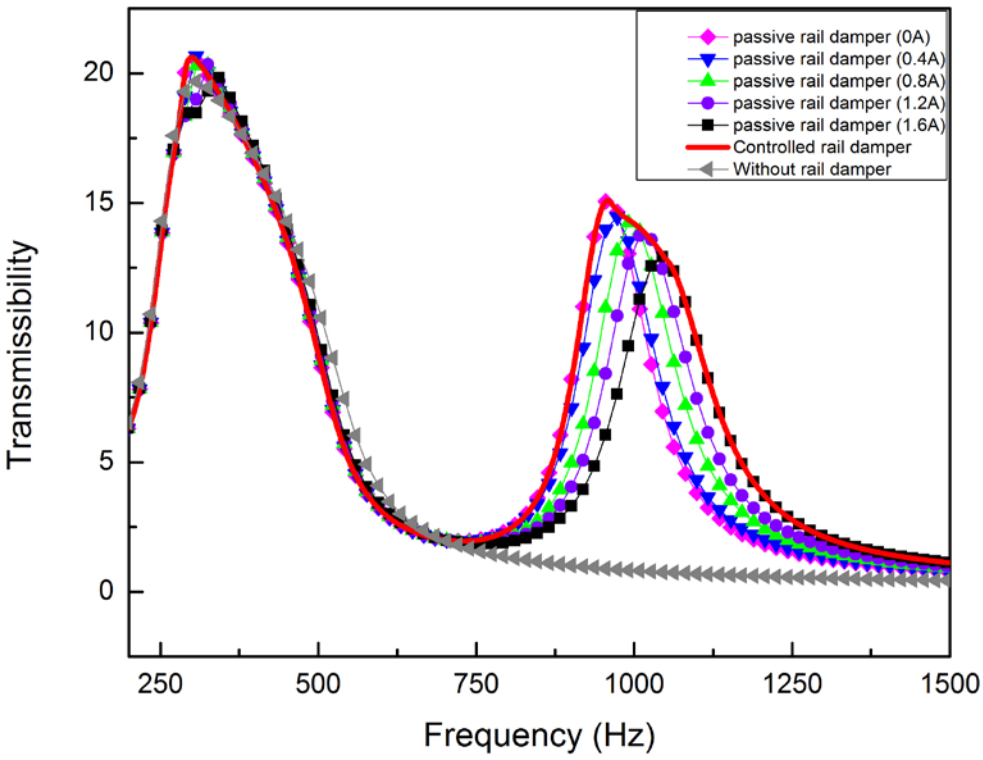

Figure 6. Estimated TDR for untreated rail and rail mounted with rail dampers

5. Conclusion

A two-mass MRE rail damper was successfully designed. Finite element analysis (FEA) verified a strong enough magnetic flux could be generated internally within the device. Moreover, the experimental characterisations of the device verified that the resonance frequencies of the rail damper can be shifted and controlled by the excitation currents. To further validate the efficiency of the device, numerical evaluation of the MRE rail damper on rail noise and vibration control using the identified parameters were conducted; it was found that the MRE rail damper could significantly expand the effective frequency bandwidth comparing with conventional rail dampers. This has great potential for reducing wayside noise emissions commonly associated with rolling noise. This research proves that the integration of variable stiffness MR technology to rail damper is promising to enhance rail damper's capability to suppress rail noise and vibration.

Acknowledges

This research is supported by ARC Linkage Grant (LP150100040) and UOW-EIS strategic research partnerships grant.

References

[1] C. Talotte, P. E. Gautier, D. J. Thompson, and C. Hanson, "Identification, modelling and reduction potential of railway noise sources: a critical survey," Journal of Sound and Vibration, vol. 267, pp. 447-468, 2003.
[2] D. J. Thompson and P. E. Gautier, "Review of research into wheel/rail rolling noise reduction," Proceedings of the Institution of Mechanical Engineers, Part F: Journal of Rail and Rapid Transit, vol. 220, pp. 385-408, 2006.
[3] D. J. Thompson and C. J. C. Jones, "A Review of the Modelling of Wheel/Rail Noise Generation," Journal of Sound and Vibration, vol. 231, pp. 519-536, 2000.
[4] J. Oertli, "The STAIRRS project, work package 1: a cost-effectiveness analysis of railway noise reduction on a European scale," Journal of Sound and Vibration, vol. 267, pp. 431-437, 2003.
[5] C. J. C. Jones, D. J. Thompson, and R. J. Diehl, "The use of decay rates to analyse the performance of railway track in rolling noise generation," Journal of Sound and Vibration, vol. 293, pp. 485-495, 2006.
[6] D. J. Thompson, C. J. C. Jones, T. P. Waters, and D. Farrington, "A tuned damping device for reducing noise from railway track," Applied Acoustics, vol. 68, pp. 43-57, 2007.
[7] X. X. Bai, N. M. Wereley, and W. Hu, "Maximizing semi-active vibration isolation utilizing a magnetorheological damper with an inner bypass configuration," Journal of Applied Physics, vol. 117 , 288, 2015.
[8] H.X. Deng, X.L. Gong, and L.H. Wang, "Development of an adaptive tuned vibration absorber with magnetorheological elastomer," Smart materials and structures, vol. 15, N111, 2006.
[9] X. M. Dong, M. Yu, S. L. Huang, Z. Li, and W. M. Chen, "half car magnetorheological suspension system accounting for nonlinearity and time delay," international Journal of Modern Physics B, vol. 19, 0503033, 2008.
[10] S. A. A. Aziz et al., "Effects of multiwall carbon nanotubes on viscoelastic properties of magnetorheological elastomers," Smart Materials & Structures, vol. 25, 077001, 2016.
[11] N. Hoang, N. Zhang, and H. Du, A dynamic absorber with a soft magnetorheological elastomer for powertrain vibration suppression. Smart materials and structures, 18, 074009, 2009.
[12] H.X. Deng, X.L. Gong, and L.H. Wang, "Development of an adaptive tuned vibration absorber with magnetorheological elastomer," Smart Materials and Structures, vol. 15, N111-N116, 2006.
[13] S.Sun, et al., The development of an adaptive tuned magnetorheological elastomer absorber working in squeeze mode. Smart Materials and Structures, 23, 075009, 2014.
[14] Y. Li, J. Li, W. Li, and B. Samali, "Development and characterization of a magnetorheological elastomer based adaptive seismic isolator," Smart Materials and Structures, vol. 22, 035005, 2013.
[15] M. Behrooz, X. Wang, and F. Gordaninejad, "Modeling of a new semi-active/passive magnetorheological elastomer isolator," Smart Materials & Structures, vol. 23, 045013, 2014.
[16] J. Fu, X. Zheng, M. C. Yu, B. X. Ju, and C. Y. Yang, "A new magnetorheological elastomer isolator in shear - Compression mixed mode," Journal of Intelligent Material Systems & Structures, vol. 8212, pp. 1702-1706, 2013.
[17] J.Yang, et al., A novel magnetorheological elastomer isolator with negative changing stiffness for vibration reduction. Smart materials and structures, 23, 105023, 2014.
[18] J. M. Ginder and W. F. Schlotter, "Magnetorheological elastomers in tunable vibration absorbers," in Smart Structures and Materials 2001: Damping and Isolation, 2001, pp. 103-

110.
[19]J. M. Ginder, S. M. Clark, W. F. Schlotter, and M. E. Nichols, "Magnetostrictive Phenomena in Magnetorheological Elastomers," International Journal of Modern Physics B, vol. 16, pp. 2412-2418, 2002.
[20] A. A. Lerner and K. A. Cunefare, "Performance of MRE-based Vibration Absorbers," Journal of Intelligent Material Systems and Structures, vol. 19, pp. 551-563, 2007.
[21] D. J. Thompson, C. J. C. Jones, T. X. Wu, and A. De France, "The influence of the non-linear stiffness behaviour of rail pads on the track component of rolling noise," Proceedings of the Institution of Mechanical Engineers, Part F: Journal of Rail and Rapid Transit, vol. 213, pp. 233-241, 1999.
[22] G. Schubert and P. Harrison, "Magnetic induction measurements and identification of the permeability of Magneto-Rheological Elastomers using finite element simulations," Journal of Magnetism and Magnetic Materials, vol. 404, pp. 205-214, 2016.
[23] S. Sun, J. Yang, W. Li, H. Deng, H. Du, and G. Alici, "Development of a novel variable stiffness and damping magnetorheological fluid damper," Smart Materials and Structures, vol. 24, 085021, 2015.
[24] T. X. Wu, "On the railway track dynamics with rail vibration absorber for noise reduction", Journal of Sound and Vibration, Vol. 309, pp. 739-55, 2008.
[25] H. P. Liu and T. X. Wu, "Reducing the rail component of rolling noise by vibration absorber: theoretical prediction," Proceedings of the Institution of Mechanical Engineers, Part F: Journal of Rail and Rapid Transit, vol. 223, pp. 473-483, 2009.
[26] J. Ryue, D. J. Thompson, P. R. White, and D. R. Thompson, "Decay rates of propagating waves in railway tracks at high frequencies," Journal of Sound and Vibration, vol. 320, pp. 955-976, 2009.
[27] S. Sun, H. Deng, J. Yang, W. Li, H. Du, G. Alici, et al., "An adaptive tuned vibration absorber based on multilayered MR elastomers," Smart Materials and Structures, vol. 24, 045045, 2015.